Steel and Composite Structures, *Vol. 17, No. 1 (2014) 47-67*
DOI: http://dx.doi.org/10.12989/scs.2014.17.1.047

Analytical study of slant end-plate connection subjected to elevated temperatures

F. Zahmatkesh*, M.H. Osman[1], E. Talebi[1] and A.B.H. Kueh[2]

[1] *Faculty of Civil Engineering at Universiti Teknologi Malaysia (UTM), 81310 UTM, Johor, Malaysia*
[2] *Construction Research Centre (CRC), Universiti Teknologi Malaysia (UTM), 81310 UTM, Johor, Malaysia*

(*Received August 16, 2013, Revised December 20, 2014, Accepted February 04, 2014*)

Abstract. Due to thermal expansion, the structural behaviour of beams in steel structures subjected to temperature increase will be affected. This may result in the failure of the structural members or connection due to extra internal force in the beam induced by the thermal increase. A method to release some of the thermally generated internal force in the members is to allow for some movements at the end supports of the member. This can be achieved by making the plane of the end-plate of the connection slanted instead of vertical as in conventional design. The present paper discusses the mechanical behaviour of beams with bolted slant end-plate connection under symmetrical gravity loads, subjected to temperature increase. Analyses have been carried out to investigate the reduction in internal force with various angles of slanting, friction factor at the surface of the connection, and allowable temperature increase in the beam. The main conclusion is that higher thermal increase is tolerable when slanting connection is used, which means the risk of failure of structures can be reduced.

Keywords: slant bolted end-plate connection; elevated-temperature; symmetric gravity load; friction factor; friction bolt; analytical model

1. Introduction

The search for an economical resistance method to improve the performance of steel structures due to elevated temperatures remains a challenging task that has captured the interest of structural engineers in recent decades. Nowadays, the following engineering solutions are common: increasing section area, provision of lateral supports, cooling system by air-conditioning and water, and thermal break. To find an economical structural protection method, it is necessary to focus on supports and member's behaviour at elevated temperatures. In an experimental study on the main members of a steel structure (Rodrigues *et al*. 2000), it is found that the thermal failure behaviour of members occurs in two principal steps: elastic and inelastic. In many cases, the first step is due to the initiation of failure that passes the tangential elastic modulus. Mourão and Silva (2007) found that the expansion of beams due to uniform heating is one of the primary causes of elastic failure. Yin and Wang (2004) explored the influence of this expansion by investigating the axially restrained beams under elevated temperatures by a numerical method. However, in both studies,

*Corresponding author, Ph.D. Candidate, E-mail: fa_zahmatkesh@yahoo.com

http://www.techno-press.org/?journal=scs&subpage=8 ISSN: 1229-9367 (Print), 1598-6233 (Online)

they concentrated on the beam member. Simões da Silva *et al*. (2001) in their research showed that the detail of connections plays an important role in carrying or damping thermal expansion of an axially restrained beam in steel structures. Heidarpour and Bradford (2009) found that the stiffness and rigidity of connections has relation to the amount of axial force in the beam. Yang and Tan (2012) and Al-Jabri (2011) simulated the behaviour of connections at elevated temperatures by numerical method to find logical compression and tension stiffness at connection zone in various cases, which was studied experimentally by Qian *et al*. (2008). Lin *et al*. (2013) developed a new model that has the advantages of both the simplistic and component-based forecasting features to predict the behaviour of the end-plate connection at elevated temperatures.

Recent literatures has shown that slant end plate connections (Fig. 1) can be a structural solution to protect connections and beam against primary failure due to elevated temperatures. The performance of a beam with a slant end-plate connection subjected to elevated temperatures has been investigated by Zahmatkesh and Talebi (2010), who demonstrated that an increase in temperature in the steel beam with a general vertical bolted connection can induce a huge extra axial force that decreases the capability in carrying external gravity loads. The study showed that by changing the connection to that of slanting type, this additional axial force can be damped. In a similar vein, a 2D simplification model for analytical method is presented to derive the equilibrium equations for beams with a slant end-plate connection in the presence of elevated temperatures when subjected to symmetric gravity load in the elastic region. The analytical equations are validated by experimental test.

2. Vertical and slant end-plate connection characteristics in beam subjected to temperature increase

2.1 Connections characteristics

Sketches of vertical and slant end-plate connections are shown in Fig. 2. The popularity of bolted end-plate connections is largely due to its simplicity in fabrication and installation. In general, these connections consist of end-plates that are welded to the ends of a beam in the

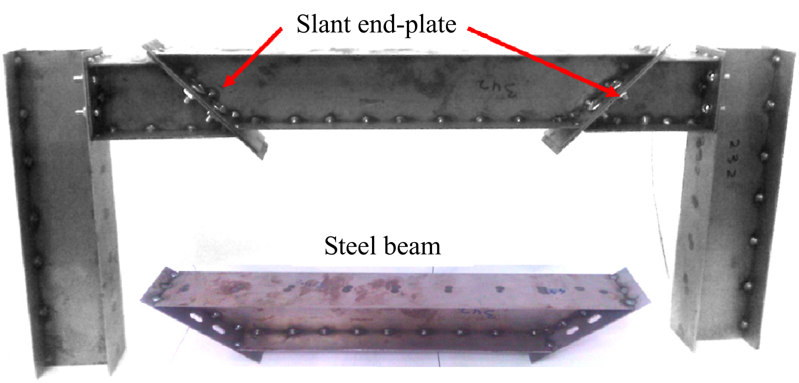

Fig. 1 A reduced scale beam with slant bolted end-plate connection

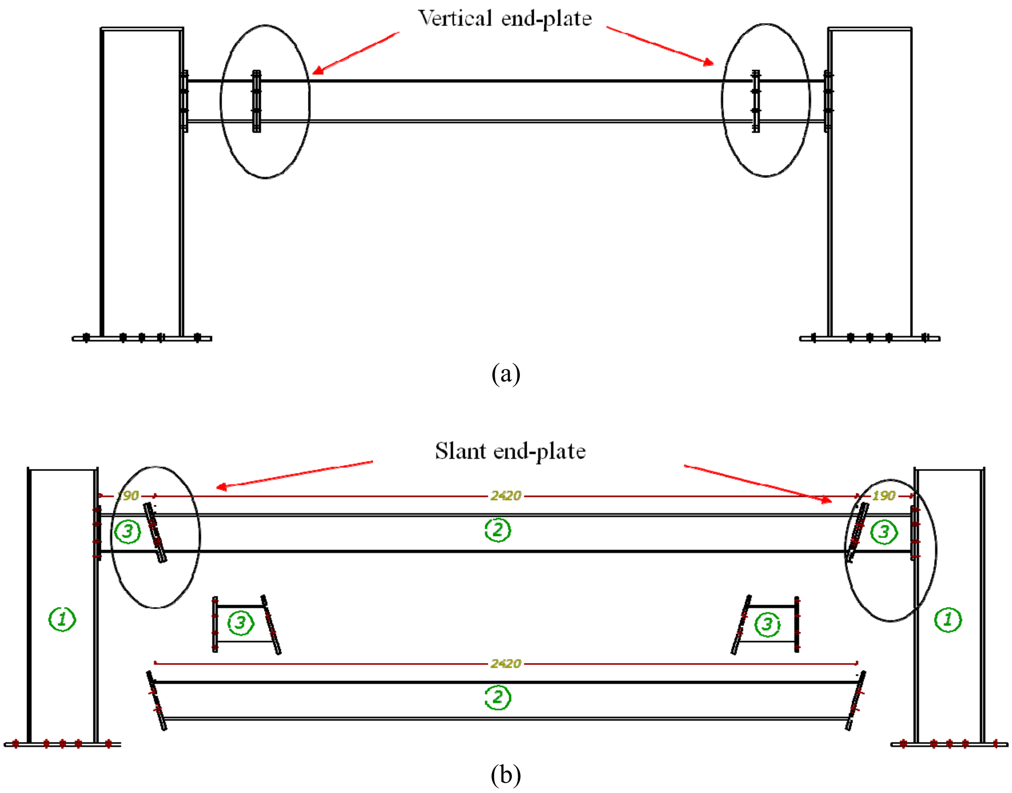

Fig. 2 Typical beam with: (a) vertical; and (b) slant bolted end-plate connections

workshop and then bolted to the flange of columns or supported end-plate on site. They are usually found in industrial structures, residential towers using knee connections with end-plate and beam connections in gable roofs. In this paper, the maximum angle of slanting of end-plate is set to 60^{o}, because a higher angle is not practical for crossing bolts into the holes at the top and bottom of the end-plate for fastening.

2.2 Damping motion of steel beam over the connection surface

The beam with restrained supports tends to have an expansion when it is subjected to temperature increase. Therefore, if the supports do not allow enough tolerance to move then their reactions will apply huge axial forces in a beam. Most of the times, the elongation of members in elastic range of material is very small, so the slant end-plate connection can damp axial force by allowing the end of a beam to crawl on the connection surface due to the elongation of the beam. Hypotheses about the stages of the performance and the reaction of end-plate connections due to increase in temperature are shown in Figs. 3 and 4, for vertical and slant types respectively. As shown in Fig. 3, in general, after an increase in temperature, the beam tends to buckle due to increase in axial load (P_{cr}), because vertical end-plate connection does not allow a beam to have expansion.

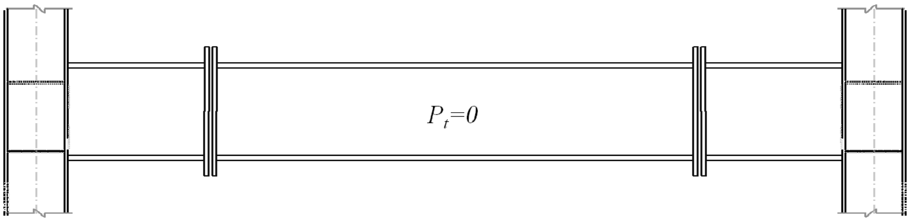

(a) Stage 1-Beam with vertical end-plate connection before increase in temperature

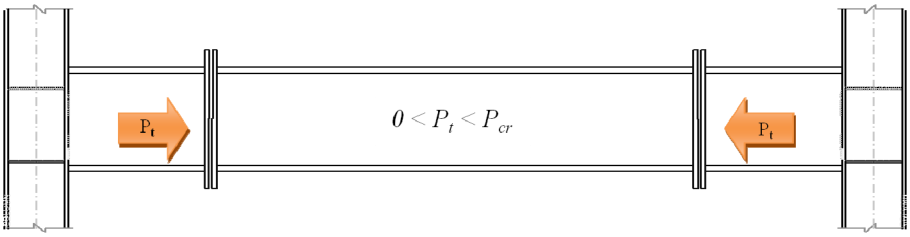

(b) Stage 2-Beam with vertical end-plate connection after increase in temperature: Two plates are in contact

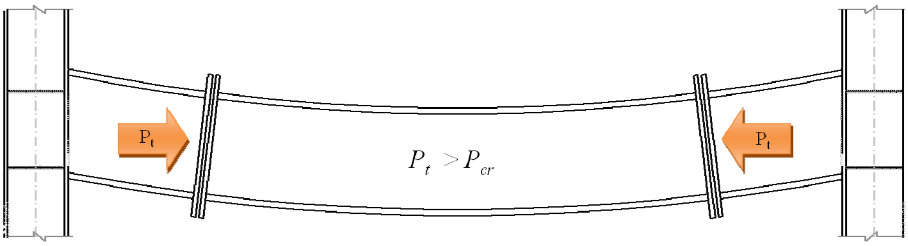

(c) Stage 3- Beam with vertical end-plate connection after increase in temperature. Buckling and decrease in Young's modulus, *E*

Fig. 3 Beam with vertical bolted end-plate connection subjected to temperature increase

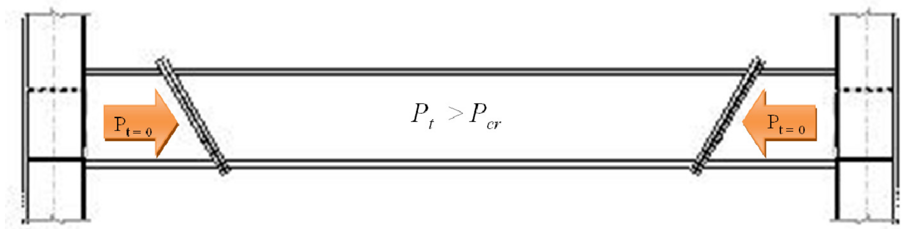

(a) Stage 1- Beam behaviour before increase in temperature

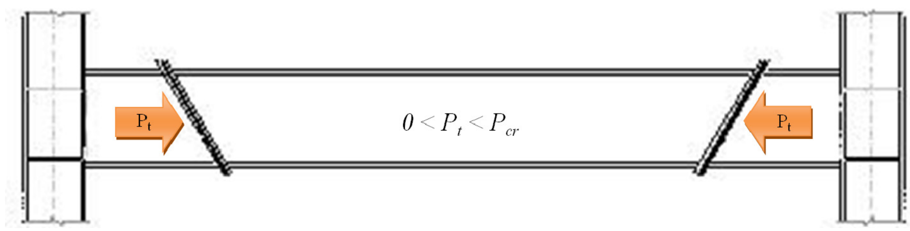

(b) Stage 2- Beam behaviour after increase in temperature: Two plates are in contact

Fig. 4 Beam with slant bolted end-plate connection subjected to temperature increase

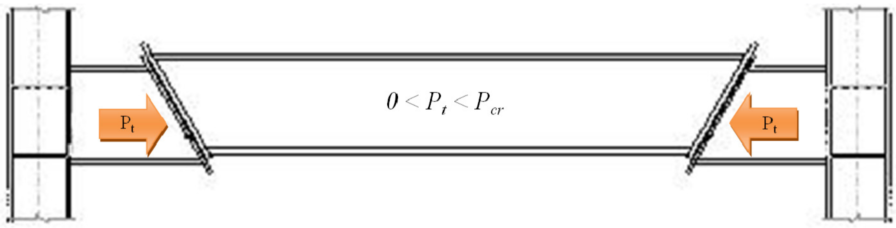

(c) Stage 3- Beam behaviour after increase in temperature: Two plates contact together and in movement

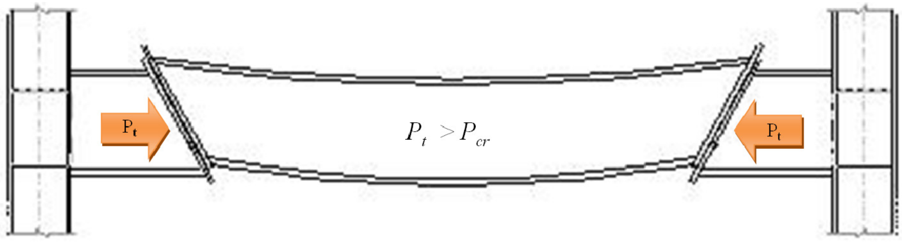

(d) Stage 4- Beam behaviour after increase in temperature: Buckling and decrease in Young's modulus, *E*

Fig. 4 Continued

On the other hand, for slant connection as shown in Fig. 4, after an increase in temperature, the supports reactions apply axial forces to the beam through member expansion such that the slant surface allows the beam to damp axial force and expansion by linear crawling on the slant surface. Although there is a vertical motion tolerance between the surfaces in vertical end-plate connections, it is unable to absorb the expansion of two ends of the beam in horizontal direction because the direction of expansion is perpendicular to the direction of moving surface. In the slant end-plate connection, there is a slanting tolerance between the surfaces such that it can absorb the expansion of two ends of the beam using crawling mechanism over the slanting faces, because the direction of horizontal expansion can be projected to the slanting plane of connection.

3. Analytical modelling formulation

3.1 Maximum allowable elevated temperatures

To simplify calculation in a two dimensional model, the joints of end-plate connections are assumed to be rigid and the supports of a beam are evaluated in three cases: firstly, roller support, secondly, friction support and thirdly, friction bolted support. As it is shown in Fig. 5, if the supports are frictionless roller on the slant plate, the beam should be in static equilibrium before thermal effect and the resulting of bending moment, M, in the two ends of the beam is equal to zero, because the beam is subjected to uniform symmetric gravity load. In static equilibrium the uniform gravity load, W, will cause roller supports tend to move downward, but the initial axial force in the beam, P_i, resists against downward movement. In this condition, if there exists compression axial force in the beam due to elevated temperatures, it would tend to move upward without any resistant force because it is frictionless. Eqs. (1) and (2) show relations between uniform gravity load, W, and the slope of connection with the normal reaction at support and axial

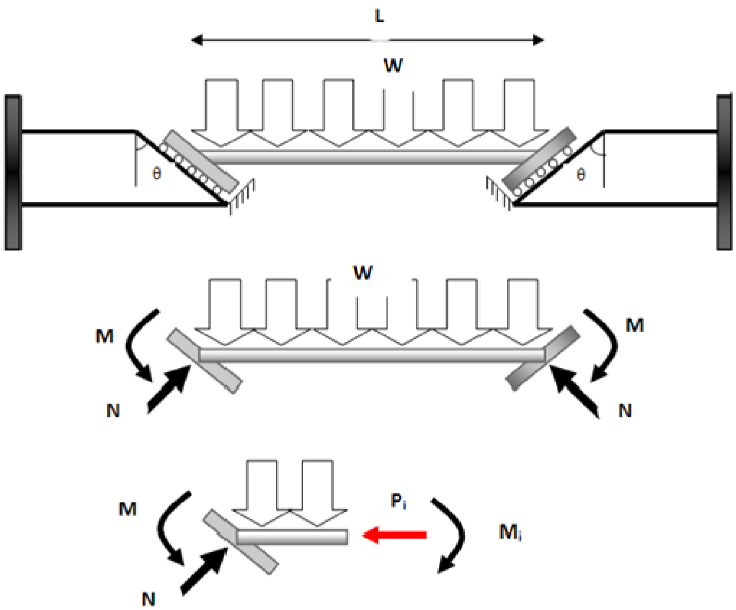

Fig. 5 Force mechanism in a beam with slant end-plate connection under thermal increase (frictionless support)

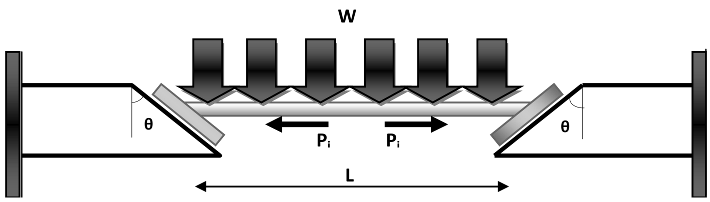

Fig. 6 Simplification model of beam with slant end-plate connection subjected to increase in temperature (friction support)

force in the beam.

$$\sum F_y = 0 - \quad \rightarrow \quad N = \frac{WL}{2\sin\theta} \tag{1}$$

$$\sum F_x = 0 - \quad \rightarrow \quad P_i = \frac{WL}{2}\cot\theta \tag{2}$$

In the second case, as shown in Fig. 6, it is supposed that the reaction of supports depends on the friction factor between two faces of joint plate. Before the thermal effect (Fig. 7), the friction force resists against downward movement. After an increase in temperature, as it is shown in Fig. 8, the beam tends to have an elongation, but there is a resistance force against the elongation; the friction force vertical component resists against upward movement. Hence, from Eqs. (3-6) the minimum requirement of axial force due to elevated temperatures can be obtained.

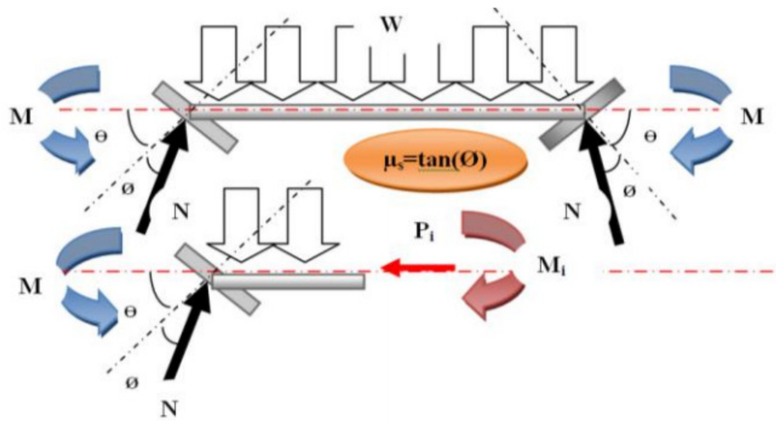

Fig. 7 Free body diagram before thermal effect (friction support)

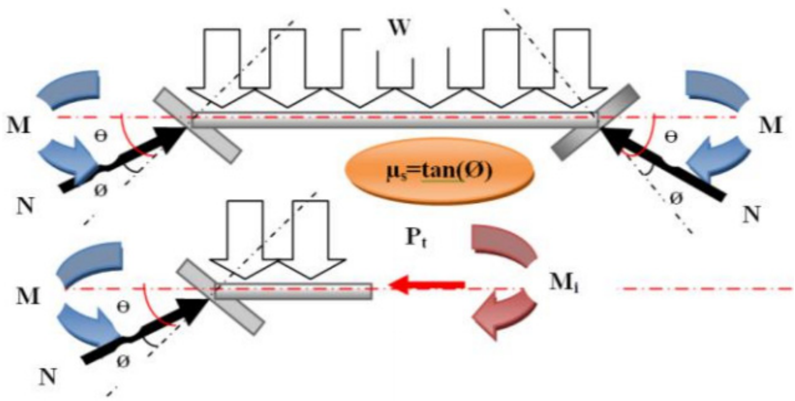

Fig. 8 Free body diagram after increase in temperature (friction support)

From Fig. 7, the equilibrium equations before the elevated temperatures on the beam can be written as

$$\sum F_y = 0 - \rightarrow N = \frac{WL}{2\sin(\theta + Ø)} \tag{3}$$

$$\sum F_x = 0 - \rightarrow P_i = \frac{WL}{2}\cot(\theta + Ø) \qquad \text{(with friction) (4)}$$

From Eq. (4), the initial axial force in the beam can be obtained.

Fig. 8 shows the free body diagram of the beam after elevated temperatures. The equilibrium equations after an increase in temperature in the beam can be written as

$$\sum F_y = 0 - \rightarrow N = \frac{WL}{2\sin(\theta - Ø)} \tag{5}$$

$$\sum F_x = 0 - \quad \rightarrow \quad P_i = P_{t\,(\text{movement})} = \frac{WL}{2}\cot(\theta - \text{Ø}) \tag{6}$$

In Eq. (6), the axial force P_t is the critical force at which the end of the beam is in the verge of moving, thus marked as $P_{t\,(\text{movement})}$. From the basic equation for axial force due to temperature increase (P_t), and Eq. (6), in the elastic field, we can derive the movement elevated temperatures, ΔT_m, given in Eq. (7).

$$\Delta T_m = N = \frac{WL}{2AE\alpha}\cot(\theta - \text{Ø}) \qquad \text{(with friction) (7)}$$

where ΔT_m is the minimum requirement elevated temperatures for sliding upward, A is cross section area, E is Young's modulus and α is coefficient of thermal expansion. The relationship between the angle of joining plane and the angle of friction coefficient is changed from ($\theta + \varphi$) in Eq. (4) to ($\theta - \varphi$) in Eq. (6). This is due to the fact that if the friction angle is greater than the slanting connection angle ($\varphi \geq \theta$), then the behaviour of slant end-plate connection is similar to the vertical connection, because the resistance force is bigger than the movement force.

In slant and vertical bolted connections, sometimes friction bolts are used to fasten end-plates

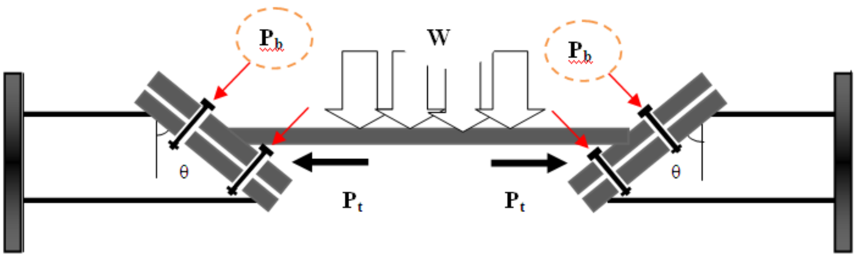

Fig. 9 Simplification model of beam with bolted slant end-plate connection due to increase in temperature

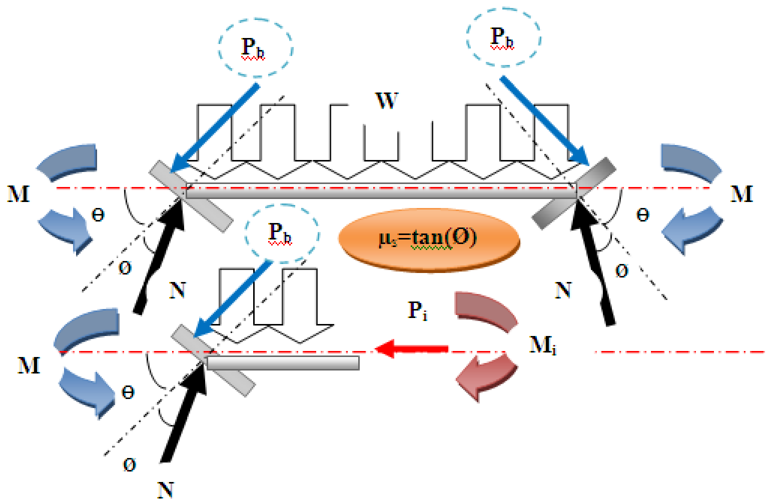

Fig. 10 Free body diagram before thermal effect (friction bolted support)

together. Therefore after calculating the required force, the external axial load is applied and controlled by force gage on the bolts to fasten the plates of connection. In the third case study, as shown in Fig. 9, it is supposed that the supports' reaction is dependent on friction factor and friction grip bolts between two faces of joint. Before the thermal increase, as shown in Fig. 10, friction force resists against downward movement. However, after applying the thermal increase, the beam tends to move upward and subsequently the friction force changes its direction to resist against upward movement (Fig. 11). In this case, the friction force resistance is stronger than the second case, because the vertical force and friction force have increased due to the fastening of bolts to resist against movement. Thus in this case the beam needs higher axial force to move upward.

From Fig. 10, the equilibrium condition before the thermal effect on the beam can be written as

$$\sum F_y = 0 - \quad \rightarrow \quad N = \frac{WL + 2P_b \sin\theta}{2\sin(\theta + \text{Ø})} \tag{8}$$

$$\sum F_x = 0 - \quad \rightarrow \quad P_i = \frac{WL + 2P_b \sin\theta}{2}\cot(\theta + \text{Ø}) + P_b \cos\theta \tag{9}$$

From Fig. 11, the equilibrium equation after the increase in temperature can be written as

$$\sum F_y = 0 - \quad \rightarrow \quad N = \frac{WL + 2P_b \sin\theta}{2\sin(\theta - \text{Ø})} \tag{10}$$

$$\sum F_x = 0 - \quad \rightarrow \quad P_{t\,(\text{movement})} = \frac{WL + 2P_b \sin\theta}{2}\cot(\theta - \text{Ø}) - P_b \cos\theta \tag{11}$$

From basic equation for axial force due to temperature increase (P_t), and Eq. (11), in the elastic field, we can obtain the movement elevated temperatures in bolted friction support, ΔT_m, i.e., the temperature increase at which the movement of beam ends start, prevented by the limited

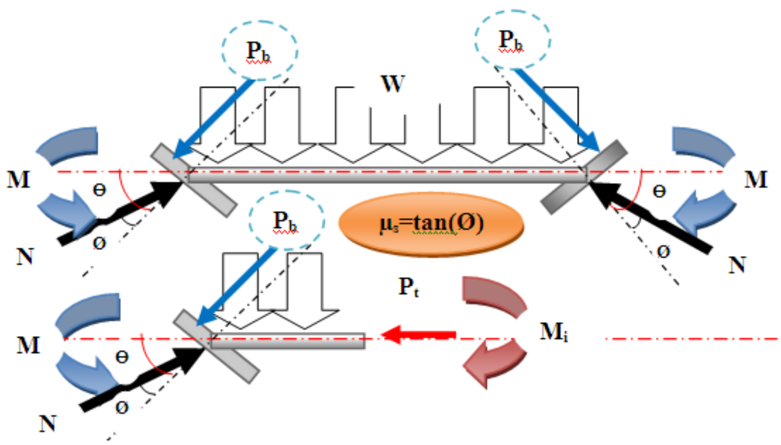

Fig. 11 Free body diagram after increase in temperature (bolted friction support)

clearance of bolt holes. This equation is given in Eq. (12) as

$$\Delta T_m = \frac{1}{\alpha AE}\left(\frac{WL + 2P_b \sin\theta}{2}\cot(\theta - \text{Ø}) - P_b \cos\theta\right) \tag{12}$$

3.2 Critical axial load in the beam-column

Assuming that in a plane frame of one structure, the beam is fixed at its joint and there are no vertical and horizontal displacements at the supports (Fig. 12). Gravity load is applied to the beam by uniform load in linear distribution form, W. From the equilibrium condition, it can be written as in Kazemi (2001): critical load, P_{cr}, and, deflection, V.

$$EI = \left(\frac{d^2v}{dx^4}\right) + P\left(\frac{d^2v}{dy^4}\right) = W(x) \tag{13}$$

After solving Eq. (13), the critical load of the beam-column from Euler formulation in buckling concept can be obtained from Eq. (14). (k is effective length factor)

$$P_{cr} = \left(\frac{\pi^2 EI}{k^2 L^2}\right) \tag{14}$$

As it is shown in Fig. 13:

If (reference temperature + increase in temperature, ΔT) < 100°C.

From the basic equation for axial thermal force (P_t) and Eq. (14) in the elastic field, the critical elevated temperatures of beam buckling (Eq. (15)) can be obtained.

$$\Delta T_{cr} = \frac{1}{\alpha}\left(\frac{\pi r}{kL}\right)^2 = \frac{1}{\alpha}\left(\frac{\pi}{\lambda}\right)^2 \tag{15}$$

where $\lambda = kL / r$ and r is slenderness ratio.

Sometimes in beam-columns, which are subjected to axial force and bending moment, before buckling of beam-column, the member can be yielded depending on slenderness ratio λ, and

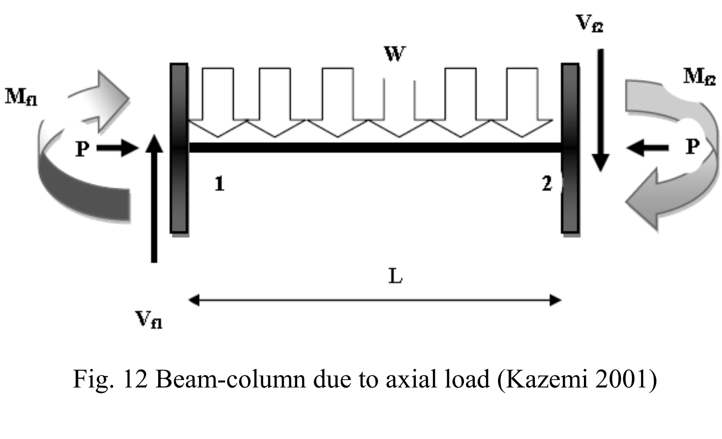

Fig. 12 Beam-column due to axial load (Kazemi 2001)

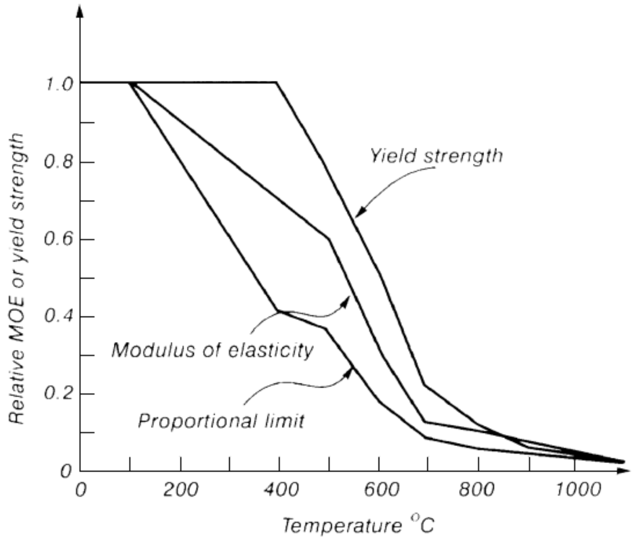

Fig. 13 Reduction in yield strength and modulus of elasticity of steel with temperature (EC3 1995)

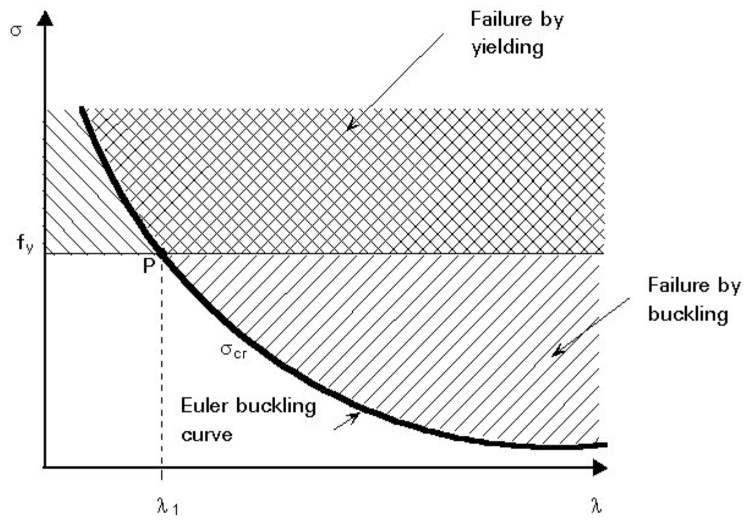

Fig. 14 The relationship between buckling strength and slenderness ratio depends on the support conditions at the column ends. (Farshi and Kooshesh 2009)

properties of section (Fig. 14). From Eq. (16), we can obtain allowable axial yielding load, P_y, by substitution of allowable yielding stress due to axial load, F_a, and bending moment, F_b, in this equation. In Eq. (16) applied stresses due to axial load, f_a, and bending moment, f_b, are various and change by external loads.

$$\frac{f_a}{F_a} + \frac{f_b}{F_b} \le 1 \tag{16}$$

Table 1 The condition of thermal movement axial force for upward sliding

If $P_y \leq P_{cr} \leq P_{t\,(\mathrm{movement})}$ beam will yield	If $P_{cr} \leq P_y \leq P_{t\,(\mathrm{movement})}$ beam will buckle	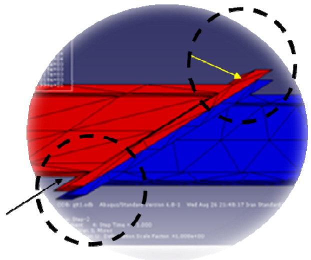 if $P_{t\,(\mathrm{movement})} \leq P_{cr} \leq P_y$ beam will move upward

As it is shown in the basic equation for thermal axial force (P_t), and Eq. (14), P_{cr} and P_t can be obtained separately. Axial load produced by temperature increase, P_t, is equal to, P_{cr}, when the amount of increase in temperature plus ambient temperature is less than 100°C, because the effect of modulus of elasticity in steel structure is linear and elastic within this temperature. Critical elevated temperatures can be obtained from Eq. (15), which as it is shown in this equation, with the increase in slenderness ratio, λ, of beam-column, the ability of strength against elevated temperatures will be reduced and exceed the critical temperature. Reduction factor should be applied to amount of elasticity modulus that is approaching to inelastic limitation.

In conventional end-plate connections (vertical plate), after an increase in temperature the beam tends to yield or buckle due to increase in the axial load, because vertical end-plate connection does not allow the beam to have an elongation. However, the slant surfaces in the two ends of the beam in the slant end-plate connection, allow for the beam to damp the axial load and elongation with linear crawling on slant surface. From the basic equation for axial force from temperature (P_t), and Eqs. (14) and (16), it can be found that if $P_{cr,}$ and P_y, are less than $P_{t\,(\mathrm{movement}),}$ then the beam will yield or buckle (Table 1). On the other hand, if $P_{cr,}$ and P_y, are higher than $P_{t\,(\mathrm{movement})}$, then the beam will move upward before buckling and additional axial load due to elongation will be damped (Table 1).

4. Comparison of analytical formulation results with experimental tests

The structural responses computed by the analytical simulation are first validated with experimental results. Experimental data were taken from small scale steel beam and frame tests carried out at the Faculty of Civil Engineering of Universiti Teknologi Malaysia (UTM). The geometrical details for the considered structure are shown in Fig. 15. As shown, H sections with a thickness of 1.5 mm were employed for beam and columns. The height of columns and the beam's length of 235 mm and 450 mm were considered, respectively.

Fig. 16 shows the composition of components used in the experimental study. The structure consists of five separate parts: two columns, two short side beams and a middle beam with two inclined ends. These five parts were assembled by normal bolts and nuts.

For the tests, the side beams and middle beam were detached as separate components from the main frame, resembling those of the analytical assumptions. The slant end-plate connection can

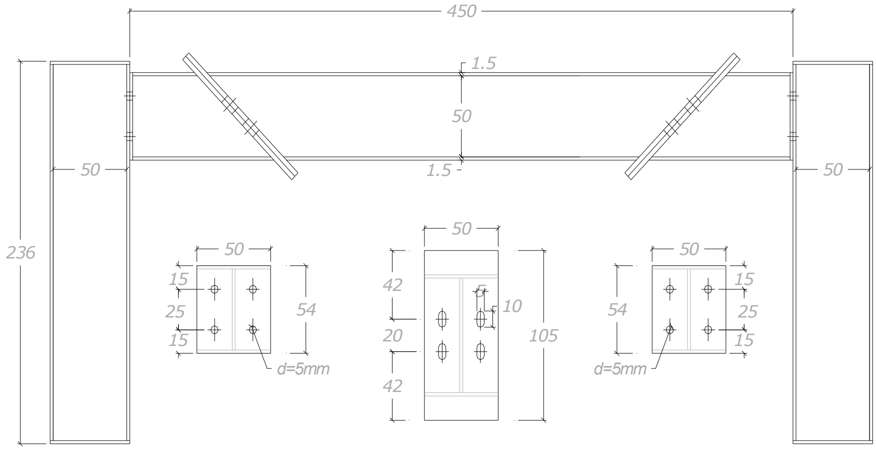

Fig. 15 Geometrical details of the slant end-plate connection in a beam-to-column for experimental study

Fig. 16 Parts of frame with slant end-plate connection used in the experimental study

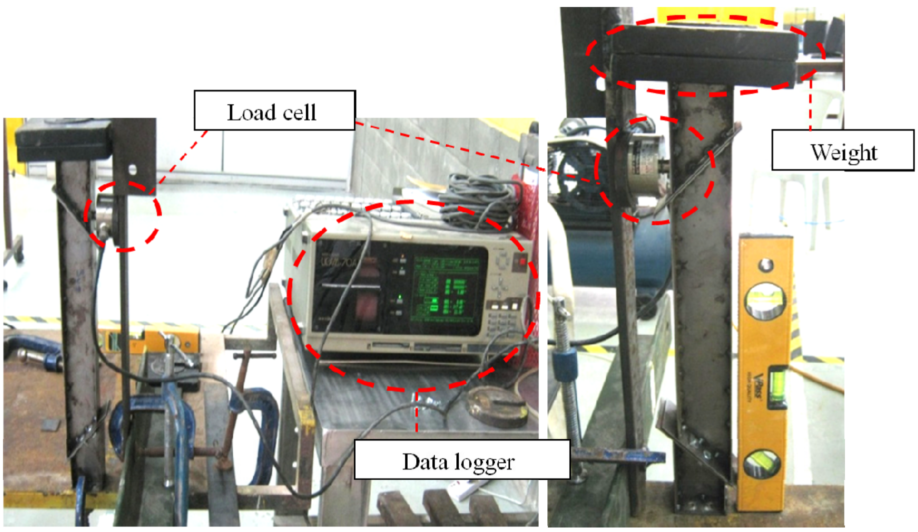

Fig. 17 Basic test for finding the static friction factor (μ_s) between two faces of slant end-plate connection

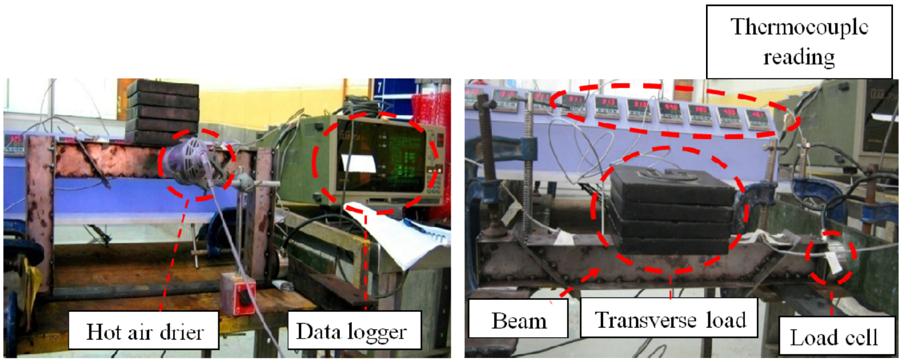

Fig. 18 Thermal test set-up

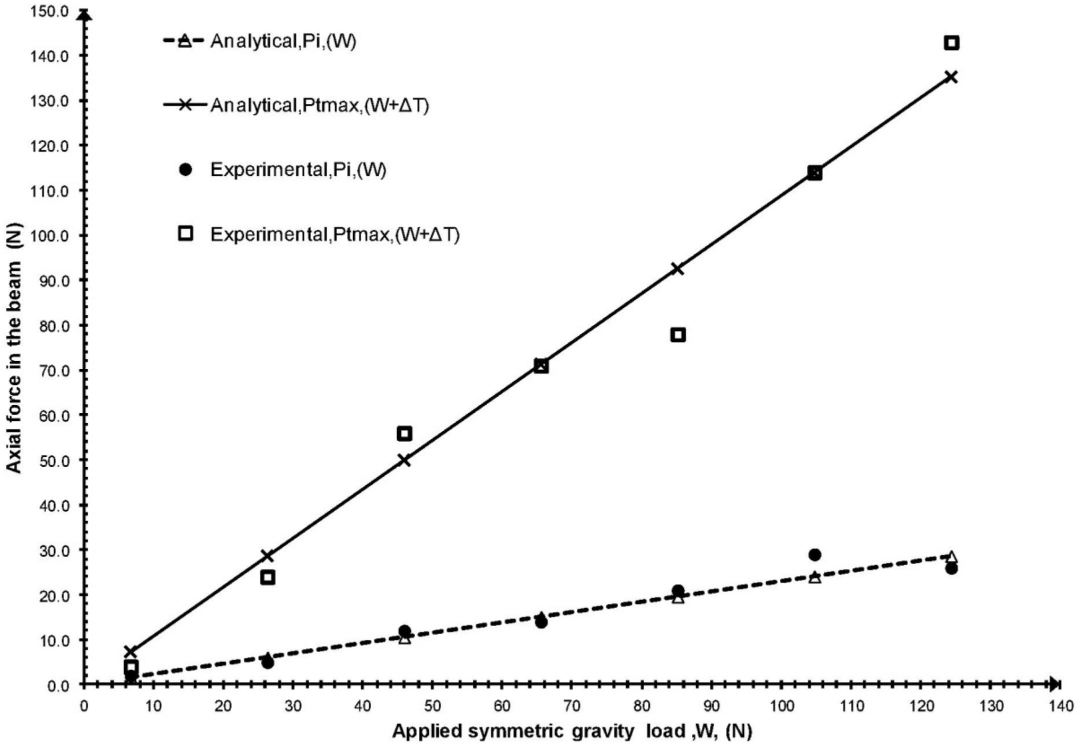

Fig. 19 The relationship between gravity load and axial force in the beam (friction factor, $\mu_s = \tan \Phi = 0.37$, $\theta = 45°$)

damp thermal axial force by motion on slant surface, so in the experimental model the holes on the slant end-plate connection were constructed such that they were of oval shape to allow this deformation. According to analytical equations, the friction factor, μ_s, between two faces of slant end-plate connection joint is desired. Subsequently, a basic test was conducted to determine this. Fig. 17 shows the test set-up. The self-weight of the beam was 0.00667 kN with a connection slanting angle of 45° ($\theta = 45°$). A 0.03922 kN attachment weight was used on the top of the side beam in the vertical position. To measure the amount of sliding force, a load cell with 50 kA- 5 kN capability was located at the side of the beam. An automated data logger (UCAM-70A) was used to measure the corresponding axial force. The basic test measured a magnitude of 0.37 ($\mu_s = \tan \varphi$) for the static friction factor of the inclined surfaces.

After the determination of the friction factor, two additional tests; before and after elevated temperatures, were carried out for measuring the structural performance of the current connection system. The set-up can be seen in Fig. 18. The beam was tested in six load intensities (0.019 kN, 0.039 kN, 0.059 kN, 0.078 kN, 0.098 kN and 0.117 kN). Similar to the basic test, axial force was recorded using the data logger with a load cell located at the end of the beam. To measure the applied temperature, 10 channels thermocouple set was attached along the beam with the heat source coming from a hot air drier placed at the middle of the beam. Note that Eqs. (4) and (6) from the model with the friction support assumption are specifically employed to produce the analytical results for comparison with experimental responses. The relationships between applied load and the amount of axial force in the beam for the investigated two cases are shown in Fig. 19. It is evident that the analytical model conforms acceptably to the outcomes produced by experiments, both before and after temperature increase, thus validating the applicability of the current analytical simulation.

5. Illustration and discussion

The structural model described in the previous section is used to analyse a steel beam section subjected to elevated temperatures, in which an IPE 300 beam is connected at both ends to slant fixed end-plate supports (Fig. 6). For the beam: cross section area, A = 5380 mm^2, modulus of elasticity, E = 210 kN/mm^2, ambient temperature, T_0 = 20°C, elevated temperatures, ΔT = 50°C, length of beam, L = 6000 mm, coefficient of thermal expansion, $\alpha = 1.5\times10^{-5}$/°C, uniformly distributed symmetric gravity load, W = 20 kN/m for the full length of span, and axially applied load on friction bolts, P_b = 50 kN (total force). The slope of slant end-plate connection (θ) and friction coefficient factor ($\mu_s = \tan \varphi$) are varied.

5.1 Axial force in beam with varying friction factor at supports

Variation in induced axial force in the beam with a slope of slant connection, θ, due to symmetric-gravity load and elevated temperatures are analysed and comparisons are made for the following conditions of loadings:

(1) Under symmetric-gravity load only, (W), where W = 20 kN/m.
(2) Symmetric-gravity load and temperature increase, ($W + \Delta T$), where ΔT = 50°C.
(3) Symmetric-gravity load and friction grip force at the bolts, ($W + P_b$), P_b = 50 kN.
(4) Combination of symmetric-gravity load, thermal increase and friction grip force, ($W + P_b + \Delta T$).

The friction coefficient factor is varied from frictionless $\mu_s = 0$ to $\mu_s = 0.2$, $\mu_s = 0.3$, and $\mu_s = 0.5$. For frictionless support, the result is shown in Fig. 20. The axial force due to symmetric-gravity load and increase in temperature are equal for all cases, because the supports are frictionless, so after substitution of friction factor ($\mu_s = 0$), in Eqs. (4), (6), (9) and (11), the same results are obtained. It is found that by increasing the angle of slanting of the connection plate, the axial force reaction decreases.

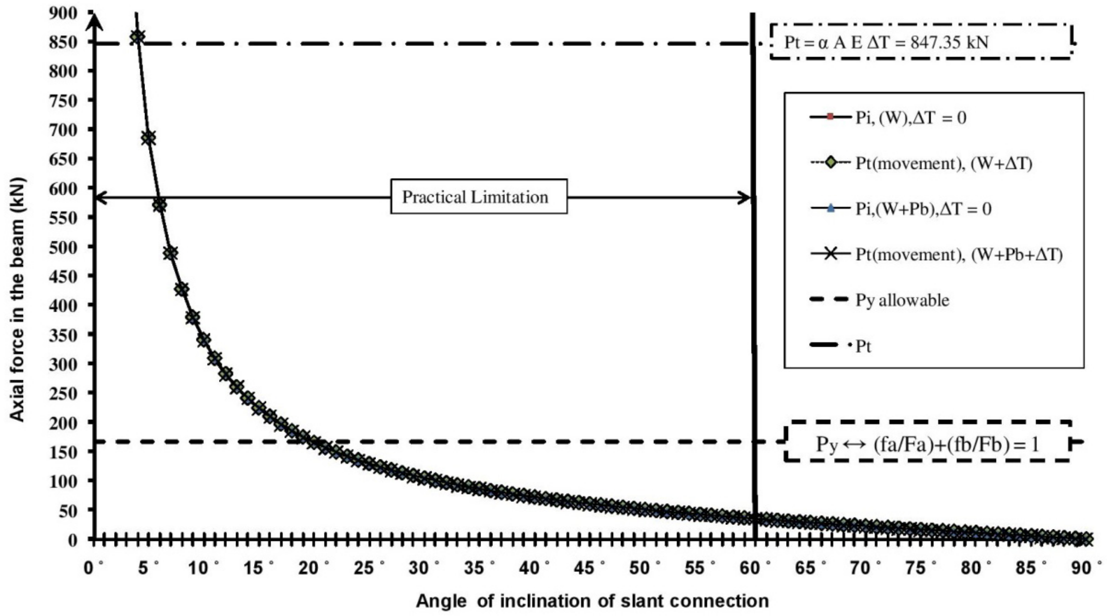

Fig. 20 Relation between axial force in the beam with the slope of slant connection ($\theta°$) due to symmetric gravity load and elevated temperatures (friction factor, $\mu_s = \tan\varphi = 0$) (ΔT) = 50°C

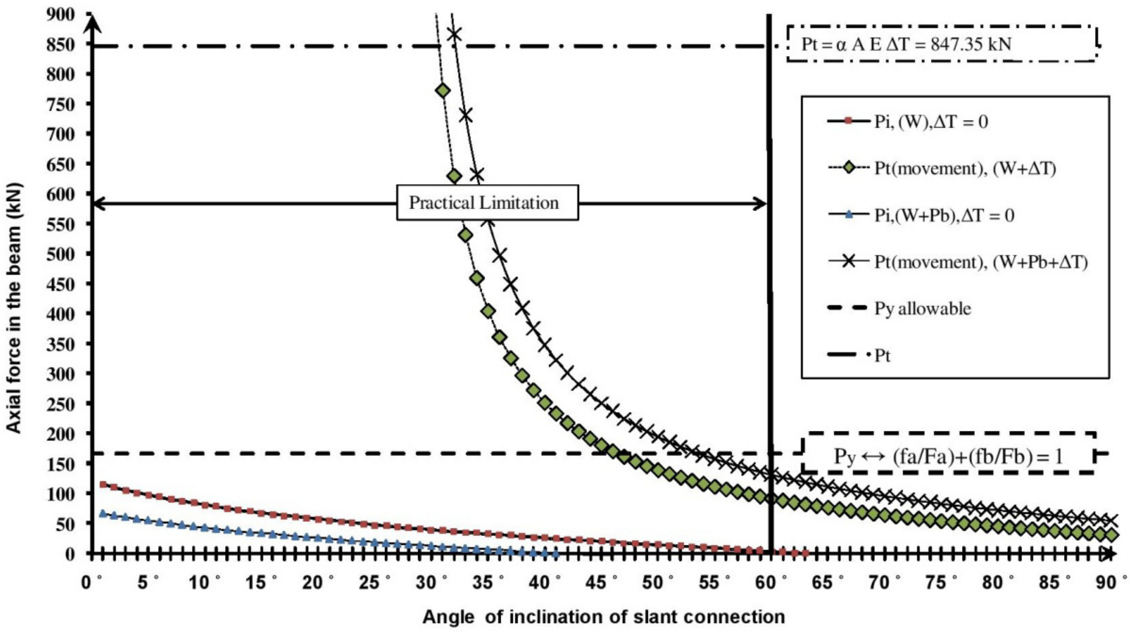

Fig. 21 Relation between axial force in the beam with the slope of slant connection ($\theta°$) due to symmetric gravity load and elevated temperatures (friction factor, $\mu_s = \tan\varphi = 0.5$) ($\Delta T$) = 50°C

It is worthwhile noting that if the slant angle is approaching zero, the beam's axial force increases to infinity (Fig. 20). Compressive arch action can be however generated and transmitted from the bottom flange at the end-plate locations to that of the top of the middle span, due to geometrical effect, thus not rendering axial force to infinity. Since the current formulation does not include such consideration, the axial force is infinitely growing because of zero slanting angle.

On the other hand where there is friction factor between two faces of connection, the results of axial force due to elevated temperatures and gravity load vary. Fig. 21 shows the result when there is friction between surfaces of slant end-plate connection, (μ_s = 0.5).

The graph in Fig. 21 shows that the axial force, due to symmetric-gravity load before any thermal effect (P_i, W) starts from 120 kN for vertical connection and decreases by increasing the angle of slant connection. It goes to zero when the angle of slant connection is equal to 63°. However, when friction bolts are used (P_i, $W + P_b$), the axial force starts from 70 kN in vertical position and goes to zero when the angle of slant connection is equal to 41°. Therefore, it is found that the amount of axial force in the beam before elevated temperatures due to symmetric-gravity load can only be decreased by friction grip bolts. After an increase in temperature, the minimum requirement of axial force in the beam for initiation of crawling ($P_{t\,(\mathrm{movement})}$, $W + \Delta T$) begins from infinity, in which the angle of the end-plate is in a vertical position, and it decreases with the increase in the angle of slant connection. The minimum requirement of axial force in the beam for initiation of crawling ($P_{t\,(\mathrm{movement})}$, $W + \Delta T$), is 90.87 kN when the angle of slanting is equal to 60° (maximum practical angle). As illustrated in this graph, when a friction bolt is used, the minimum requirement of axial force in the beam for initiation of sliding ($P_{t\,(\mathrm{movement})}$, $W + P_b + \Delta T$), is higher than the case of general bolted connection ($P_{t\,(\mathrm{movement})}$, $W + \Delta T$). Therefore if a friction bolt is used instead of general bolts, the beam needs higher axial force due to elevated temperatures to start crawling on the slant plane. The friction grip bolts can be useful for decreasing the induced axial force in the beam before any thermal effect. However, if we do not consider the damping behaviour of the bolted slant end-plate connection, it can be harmful when it is subjected to temperature increase. This is indicated in Fig. 21, i.e., by increasing the normal force of the friction bolt, the minimum requirement of axial force in the beam for the start of sliding ($P_{t\,(\mathrm{movement})}$, $W + P_b + \Delta T$), will increase. In certain range, before any crawling at two ends of the beam on the slant connection surface, the beam will start to yield or buckle first. Fig. 22 shows the relation between axial force in the beam with slope of slant connection (θ°) due to symmetric gravity load and elevated temperatures with friction factor, $\mu_s = \tan \varphi = 0.3$. As can be seen in the graph, before thermal effect, the axial force starts from 200 kN when the beam is subjected to gravity load only (P_i, W), and 150 kN when the beam is subjected to gravity load combined with the effect of the friction grip bolts force (P_i, $W + P_b$).

In these two cases the force goes to zero when the connections angles are 73° and 59°, respectively. Thus, without thermal increase, the influence of the friction bolts on decreasing induced axial force is similar to the previous case ($\mu_s = tan\ \varphi = 0.5$). Also, a comparison of Fig. 21 and Fig. 22 shows that, by decreasing friction factor, μ_s, from 0.5 to 0.3, the induced axial force increases. After the increase in temperature the minimum requirements of axial force in the beam for the start of crawling for both cases ($P_{t\,(\mathrm{movement})}$, $W + \Delta T$ and $W + P_b + \Delta T$), when the angle of end-plate connection is 60°, are 63.6 kN, and 84.6 kN, respectively. Hence, in comparison with the previous case (μ_s = 0.5), the minimum requirement of axial force in the beam for initiation of crawling decreases, i.e., the beam will start to crawl on slant plane under lesser initial axial force.

Fig. 23 shows the relation between axial force in the beam with slope of slant connection (θ°) due to symmetric-gravity load and elevated temperatures with effective friction factor,

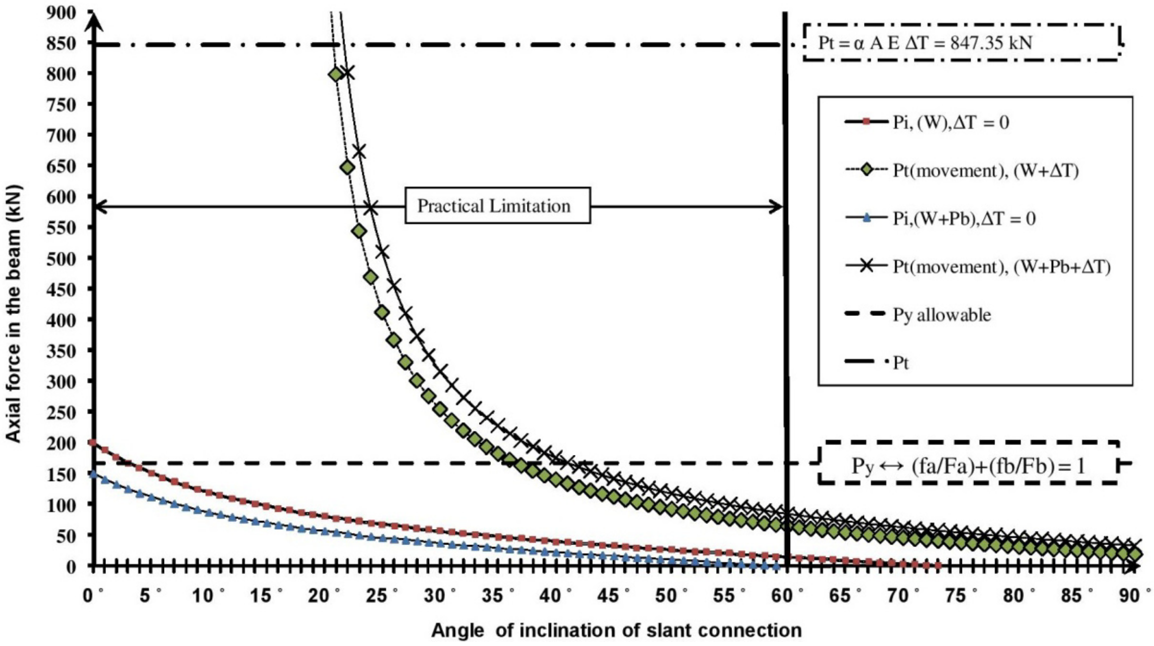

Fig. 22 Relation between axial force in the beam with the slope of slant connection ($\theta°$) due to symmetric gravity load and elevated temperatures (friction factor, $\mu_s = \tan \varphi = 0.3$) ($\Delta T$) = 50°C

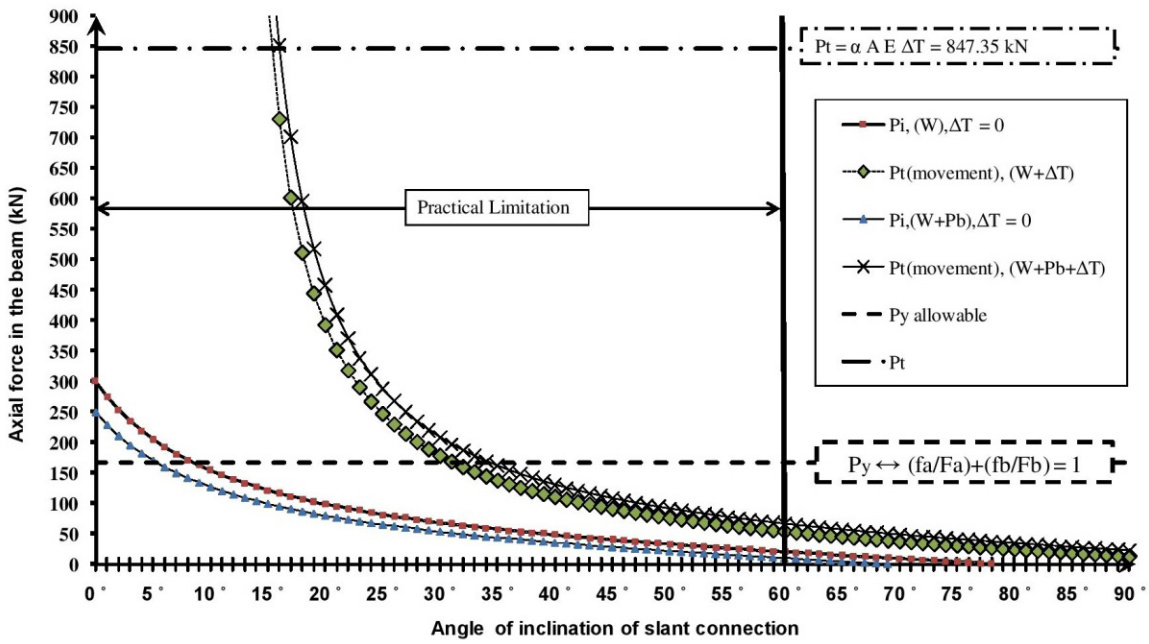

Fig. 23 Relation between axial force in the beam with the slope of slant connection ($\theta°$) due to symmetric gravity load and elevated temperatures (friction factor, $\mu_s = \tan \varphi = 0.2$) ($\Delta T$) = 50°C

μ_s = tan φ = 0.2. As shown in this figure, the same result can be obtained about the relation between reduction of friction factor and increasing induced axial force before elevated temperatures, and also the relation between reduction of friction factor and decreasing the minimum requirement axial force in a beam for initiation of crawling.

5.2 Movement elevated temperatures

Variation of increase in temperature, ΔT_m, in the beam with a slope of slant connection, θ, due to symmetric gravity load and normal force of friction bolt, is shown in Fig. 24. For μ_s = 0, the thermal increases are similar for all cases. After substitution of friction factor (μ_s = 0), in Eqs. (7) and (12), the same results can be obtained and it is found that by an increase in the angle of connection from vertical to slant position, the thermal increase at movement, ΔT_m, in the beam on the slant plane of connection will decrease. When approaching to vertical connection (conventional form of connections), the required elevated temperatures for the movement goes to infinity. Fig. 13 shows that, the behaviour of a steel member in the elastic field subjected to elevated temperatures is limited to 100°C, so the maximum elevated temperatures in this illustration with ambient temperature 20°C cannot exceed 80°C. In the case where there is friction between two faces of connection plates, the movement elevated temperatures, ΔT_m, under normal force of friction bolt varies. Referring to the graph, if the angle of the end plate, θ, is equal to the angle of friction factor, φ, then the movement elevated temperatures, ΔT_m, in the beam goes to infinity. From the graph, it is indicated that when the end-plate approaches vertical position, the elevated temperatures required for the movement approaches infinity. On the other hand, if the end-plate

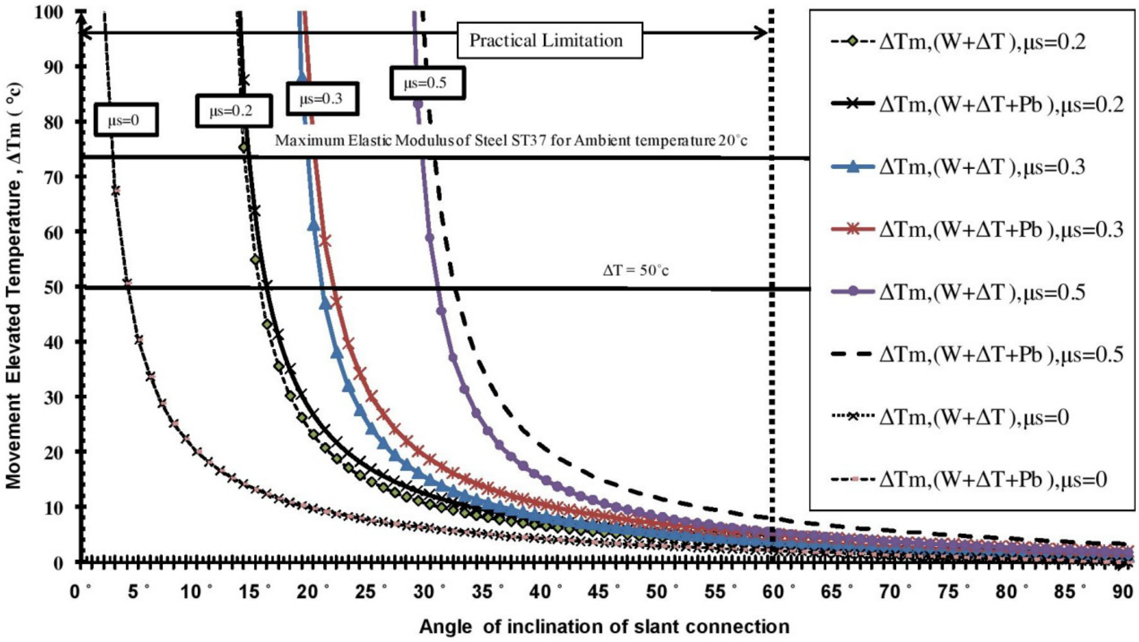

Fig. 24 Relation between movement elevated temperatures, ΔT_m, and slope of slant connection (θ°) under symmetric gravity load

inclination approaches horizontal position, the required thermal increase approaches ero. It is also shown that by increasing the friction factor from zero to 0.5, the amount of minimum elevated temperatures for movement, ΔT_m, increases, which means that the friction force resists against upward crawling at the end of the beam and it needs higher elevated temperatures to start moving. As regards the effect of gripping force P_b, it requires higher thermal increase for the beam ends to move.

6. Conclusions

This paper discussed the development of linear analytical modelling of the beam with bolted slant end-plate connection at both ends subjected to uniform temperature increase and symmetric gravity load. The thermal force is the primary cause of decrease in strength of the restrained beam under applied loads. By changing the connections' detail from vertical to slanting angle with slant end, the huge induced axial force can be damped by way of the sliding of the end support of the beam, which is made possible by the gap tolerance of the bolt hole.

The analytical investigation has shown that the minimum requirement of elevated temperatures for crawling at the end of the beam, ΔT_m, increases with the increase of friction resistance, because the friction force gives resistance against upward crawling of the end of beam. In the case where friction grip bolts are used, the grip normal force will provide extra friction resistance, hence the need for higher thermal increase for the movement of the beam. In application, by adjusting between symmetric-gravity load, slope of the end-plate, friction factor and the normal force of friction bolts, we can obtain the optimum design that has enough ability to absorb the huge thermal axial force, before any yielding and buckling in the beam. It is worth noting nonetheless that the structural responses investigated in the current work are applicable only for low temperature change, i.e., not under long exposure to fire. A realistic fire condition may impose numerous more subtle matters, such as a reduction in mechanical properties and the coupling effects of vertical forces. These issues may be examined in future work.

Acknowledgments

The research is based upon the work supported by the School of Graduate Studies Universiti Teknologi Malaysia (SPS).

References

Al-Jabri, K.S. (2011), "Modelling and simulation of beam-to-column joints at elevated temperature: A review", *J. Franklin Insti.*, **348**(7), 1695-1716.

European Committee for Standardization (1995), Euro Code 3, Design of Steel Structures. Part 1.2: General rules, structural fire design, ENV 1993-1-2, ECS, Brussels, Belgium.

Farshi, B. and Kooshesh, F. (2009), "Buckling analysis of structural steel frames with inelastic effects according to codes", *J. Construct. Steel Res.*, **65**(10-11), 2078-2085.

Heidarpour, A. and Bradford, M.A. (2009), "Elastic behaviour of panel zone in steel moment resisting frames at elevated temperatures", *J. Construct. Steel Res.*, **65**(2), 489-496.

Kazemi, M.T. (2001), *Structural Mechanic*, Sharif University of Technology Book, Tehran, Iran.

Lin, S., Huang, Z. and Fan, M. (2013), "Analysis of end-plate connections at elevated temperatures", *Steel*

Compos. Struct., Int J., **15**(1), 81-101.
Mourão, H.D.R. and Silva, V.P. (2007), "On the behaviour of single-span steel beams under uniform heating", *J. Brazilian Soc. Mech. Sci. Eng.*, **29**(1), 115-122.
Qian, Z.H., Tan, K.H. and Burgess, I.W. (2008), "Behavior of steel beam-to-column joints at elevated temperature: Experimental investigation", *J. Struct. Eng.*, **134**(5), 713-726.
Rodrigues, J.P.C., Cabrita Neves, I. and Valente, J.C. (2000), "Experimental research on the critical temperature of compressed steel elements with restrained thermal elongation", *Fire Safety J.*, **35**(2), 77-98.
Simões da Silva, L., Santiago, A. and Vila Real, P. (2001), "A component model for the behaviour of steel joints at elevated temperatures", *J. Construct. Steel Res.*, **57**(11), 1169-1195.
Yang, B. and Tan, K.H. (2012), "Numerical analyses of steel beam-column joints subjected to catenary action", *J. Construct. Steel Res.*, **70**, 1-11.
Yin, Y.Z. and Wang, Y.C. (2004), "A numerical study of large deflection behaviour of restrained steel beams at elevated temperatures", *J. Construct. Steel Res.*, **60**(7), 1029-1047.
Zahmatkesh, F. and Talebi, E. (2010), "The performance of bolted slant end plate connections subjected to temperature increase", *ASME 2010 10th Biennial Proceeding on Engineering Systems Design and Analysis*, Istanbul, Turkey, July, Paper No. ESDA2010-24720, pp. 207-217.

CC

Nomenclature

E	Young's modulus;	α	Coefficient of thermal expansion
I	Moment of inertia	ΔT	Additional temperature
L	Length of the beam-column;	A	Cross section of beam-column
P_{cr}	Critical compressive axial load	ΔT_{cr}	Critical additional temperature
v	Deflection function	ΔT_m	Movement temperature
α	Coefficient of thermal expansion	λ	Slenderness ratio
ΔT	Additional temperature	μ_s	Friction factor
A	Cross section of beam-column	r	Radius of gyration
ΔT_{cr}	Critical additional temperature	M	Bending moment
ΔT_m	Movement temperature	P_t	($P_t = \alpha AE\ \Delta T$) Axial force due to increase in temperature